Structure, Vol. 12, 1199–1207, July, 2004, ©2004 Elsevier Ltd. All rights reserved. DOI 10.1016/j.str.2004.04.021

Structure of a Lipid Droplet Protein: The PAT Family Member TIP47

Sabrina J. Hickenbottom,[1] Alan R. Kimmel,[1] Constantine Londos,[1] and James H. Hurley[2,*]
[1]Laboratory of Cellular and Developmental Biology
[2]Laboratory of Molecular Biology
National Institute of Diabetes and Digestive and Kidney Diseases
National Institutes of Health
U.S. Department of Health and Human Services
Bethesda, Maryland 20892

Summary

The *p*erilipin/*A*DRP/*T*IP47 (PAT) proteins localize to the surface of intracellular neutral lipid droplets. Perilipin is essential for lipid storage and hormone regulated lipolysis in adipocytes, and *perilipin* null mice exhibit a dramatic reduction in adipocyte lipid stores. A significant fraction of the ~200 amino acid N-terminal region of the PAT proteins consists of 11-mer helical repeats that are also found in apolipoproteins and other lipid-associated proteins. The C-terminal 60% of TIP47, a representative PAT protein, comprises a monomeric and independently folded unit. The crystal structure of the C-terminal portion of TIP47 was determined and refined at 2.8 Å resolution. The structure consists of an α/β domain of novel topology and a four-helix bundle resembling the LDL receptor binding domain of apolipoprotein E. The structure suggests an analogy between PAT proteins and apolipoproteins in which helical repeats interact with lipid while the ordered C-terminal region is involved in protein:protein interactions.

Introduction

Adipose triacylglycerols (TAG) comprise the primary energy reserve in animals. Excessive adipose TAG storage is associated with obesity, which in turn can lead to serious health problems, including type II diabetes. Obesity is now considered an epidemic in the United States, and its incidence continues to rise. Despite the profound importance of adipose TAG in human health, understanding the molecular regulation of TAG turnover is still in its infancy. TAG is stored within adipocytes in the form of lipid droplets. These droplets consist of a hydrophobic TAG core surrounded by a phospholipid monolayer with associated embedded proteins (Brown, 2001; Londos et al., 1999). The lipid droplets in adipocytes can be very large (>50 μm in diameter), but most cells contain small lipid droplets (<1 μm) for use as internal energy stores, precursors for membrane biogenesis, or other functions. Steroidogenic cells contain similar droplets that are enriched in cholesteryl esters (CE).

The best characterized of the specific lipid droplet-associated proteins of animals are the perilipins (Londos et al., 1999). Multiple perilipin (peri) forms are expressed as the result of the alternative splicing of a single gene transcript (Lu et al., 2001). Perilipin shares sequence similarity with the mammalian proteins ADRP (*a*dipose *d*ifferentiation-*r*elated *p*rotein) and TIP47 (*t*ail-*i*nteracting *p*rotein of 47 kDa), and together they comprise a family known as the PAT (*p*erilipin/*A*PRP/*T*IP47) proteins. Perilipin and ADRP are specifically localized to the surfaces of intracellular neutral lipid droplets (Londos et al., 1999). While TIP47 is also lipid droplet associated (Miura et al., 2002; Ohashi et al., 2003; Wolins et al., 2001), this interaction is not exclusive. TIP47 is additionally abundant through the cytosol (Barbero et al., 2001; Miura et al., 2002). The PAT proteins are similar to each through nearly their entire sequences, with the exception of an ~20 residue N-terminal extension in TIP47 and C-terminal extensions of varying length in the different perilipins. The sequence identity between the C-terminal half of perilipin and that of ADRP and TIP47 is low on a pairwise basis, but is discernable in a Hidden Markov Model-based alignment, and this region is included in the family-wide sequence alignment of PAT proteins in the Pfam database (Bateman et al., 2002). In addition to perilipin, ADRP, and TIP47, PAT protein members have been identified in species as diverse as *Dictyostelium* and *Drosophila*, and other mammalian PAT proteins have also been described. Collectively the PAT proteins share sequence similarity and localization to neutral lipid droplets in cells.

Perilipin expression is largely confined to adipocytes, whereas ADRP and TIP47 have broad tissue distributions (Brasaemle et al., 1997; Diaz and Pfeffer, 1998). Perilipin functions as a critical regulator of TAG lipolysis in adipocytes (Martinez-Botas et al., 2000; Souza et al., 1998; Sztalryd et al., 2003). Perilipin is also capable of stimulating lipolysis in transfected fibroblasts (Brasaemle et al., 2000; Souza et al., 2002; Tansey et al., 2001). In unstimulated adipocytes, lipid droplet TAG is poorly hydrolyzed by hormone-sensitive lipase (HSL). The perilipin-associated intracellular lipid droplets are thought to be inaccessible to HSL. Thus HSL is sequestered in the cytosol apart from its substrate TAG. Upon adrenergic hormone stimulation of adipocytes, adenylyl cyclase becomes activated, leading to an elevation in intracellular 3′,5′-cyclic adenosine monophosphate (cAMP) levels that activate protein kinase A (PKA). Perilipin and HSL are, in turn, phosphorylated by PKA. Phosphorylation of perilipin increases the accessibility of TAG to HSL, and translocation of HSL to lipid droplet surfaces increases lipolysis ~30-fold compared with unstimulated cells (Sztalryd et al., 2003). *peri* null mice have defects in both lipid storage and turnover (Martinez-Botas et al., 2000; Tansey et al., 2001). Adipocytes from these mice have higher basal lipolytic rates than do wild-type, but also manifest an attenuated response to hormone stimulation (Tansey et al., 2001). In consequence, the *peri* null mice exhibit a significant (~70%) reduction in stored TAG levels resulting in an overall lean phenotype. Perili-

*Correspondence: hurley@helix.nih.gov

pin may be a new potential target for molecular interventions against obesity.

The roles of ADRP and TIP47 in lipid metabolism are not as well defined as for perilipin. ADRP and TIP47 are 50% identical in sequence to each other throughout essentially their entire length, and the two proteins might therefore be expected to have similar physiological roles. However, their intracellular localizations are not identical. TIP47 is distributed at multiple sites in the cell, including lipid droplets and the cytosol (Miura et al., 2002). TIP47 was first isolated through interaction with mannose 6-phosphate receptors (MPRs) and is suggested to be involved in the trafficking of MPRs from endosomes to the Golgi (Diaz and Pfeffer, 1998). However, TIP47 is not required for trafficking of cation-dependent MPR (CD-MPR or MPR46) in mouse embryonic fibroblasts (MEFs) (Medigeshi and Schu, 2003). A connection between lipid droplet association and cytosolic localization of TIP47 (Miura et al., 2002) and its role in endosomal trafficking has yet to be resolved. In addition to the MPRs, the cytoplasmic domain of the HIV-1 glycoprotein gp41 has also been reported to interact with TIP47 (Blot et al., 2003). ADRP has no reported protein trafficking functions. ADRP has been reported to bind fatty acids and sterols (Serrero et al., 2000; Atshaves et al., 2001), and it has been implicated in cell-to-cell lipid transfer during lung surfactant biosynthesis (Schultz et al., 2002). One of the few other functionally characterized PAT proteins is LSD2 of *Drosophila*. As with the *peri*$^{-/-}$ mice, *Lsd2*$^{-/-}$ *Drosophila* have a lean phenotype as the result of decreased TAG stores (Gronke et al., 2003).

In spite of the urgency of understanding how PAT proteins interact with lipid droplets, progress has been hindered by a lack of three-dimensional structural information on this protein family. In an effort to better understand the modular architecture of PAT proteins, a series of constructs were made and assayed for solubility and aggregation. TIP47 was chosen as the model protein for this study because of its partial cytosolic localization (Diaz and Pfeffer, 1998; Miura et al., 2002) and of previous biochemical studies (Sincock et al., 2003) that indicate that TIP47 is tractable for in vitro biochemical and structural analyses. Consistent with previous reports (Sincock et al., 2003), we have found that the C-terminal ~60% of TIP47 comprises a soluble monomeric, protein domain, while the N-terminal region promotes aggregation in solution. We refer to these regions as "PAT-C" and "PAT-N," respectively. Here, we report the 2.8 Å crystal structure of the PAT-C region.

Results

Domain Structure of TIP47

Twelve mouse TIP47 variants were engineered as recombinant proteins in *Escherichia coli*, spanning all regions of TIP47 (Figure 1). Only the recombinant proteins that included the C terminus of the intact protein were in the soluble fraction following induction and cell lysis. Full-length TIP47 was soluble but formed large aggregates as judged by gel filtration analysis. C-terminal deletion of only 14 amino acids was sufficient to disrupt solubility. The shortest protein construct (191–437) that included the natural C terminus was predominantly monomeric as judged by gel filtration. It was concluded that PAT-C (residues 191–437) of TIP47 comprise an independently folding unit, and that an intact C terminus is essential for the stability of this unit. A significant portion of the N-terminal region is comprised of an 11-mer repeat region (Figure 1). A construct comprising residues 117–437, which contains all of the 11-mer repeats was also found to behave as a monomer. Interactions between the first 116 residues of the PAT-N region, which precede the 11-mer repeats, presumably are responsible for the observed aggregation (see below).

Crystal Structure of the TIP47 PAT-C Region

The structure of the PAT-C region of TIP47 was determined by multiple isomorphous replacement with anomalous dispersion (MIRAS) and density modification at 3.0 Å (Table 1). The protein structure was refined against native data to a working R factor of 0.236 and a free R factor of 0.272 at 2.8 Å (Figure 2). In view of the moderate resolution, no solvent molecules were incorporated into the model. The PAT-C region (residues 191–437) makes roughly the shape of a capital "L." The foot of the "L" consists of a compact α/β domain, while its leg consists of an elongated four-helix bundle (Figure 3). Residues 191–205, 289–320, and 432–437 could not be located in the electron density and are presumed disordered.

The most N- and C-terminal sections of the PAT-C (residues 206–247 and 419–431, respectively) interlace to form the α/β domain. This domain is roughly 30 Å across its largest dimension. The α/β domain consists of two helices and two β sheets, each consisting of two strands. One sheet is parallel, the other antiparallel. The N-terminal portion of the sequence contributes the helices and two β strands, and the C-terminal portion contributes the other two β strands. The sheets are organized are follows: sheet I is parallel and consists of β1 and β4; sheet II is antiparallel and consists of strands β2 and β3. The helical layer of the domain is distal to the four-helix bundle domain, and the β layer is proximal.

The four-helix bundle is formed by residues 248–418 and is 63 Å long from end to end. The helices range from 7 to 11 turns in length. After initial refinement, unassigned density was noted contiguous with the side chain of Cys-344. The density could be completely fit by a single molecule of β-mercaptoethanol (βME), and the structure was then refined with a single βME covalently attached to Cys-344. The electron density is broken between the end of the visible portion of the first helix in the bundle (α3) and the beginning of the second helix in the bundle (α4). Helices α3 and α4 are antiparallel and adjacent to each other, suggesting the antiparallel helical arrangement could continue beyond what can be visualized in the density. The missing residues could form up to four additional turns of each of the two helices, which would be consistent with the secondary structure in this region as predicted by the PHD server (Rost and Liu, 2003).

A deep cleft between the α/β domain and the four-helix bundle domain is the most striking feature of the PAT-C structure (Figure 4). The cleft is roughly 13 Å at

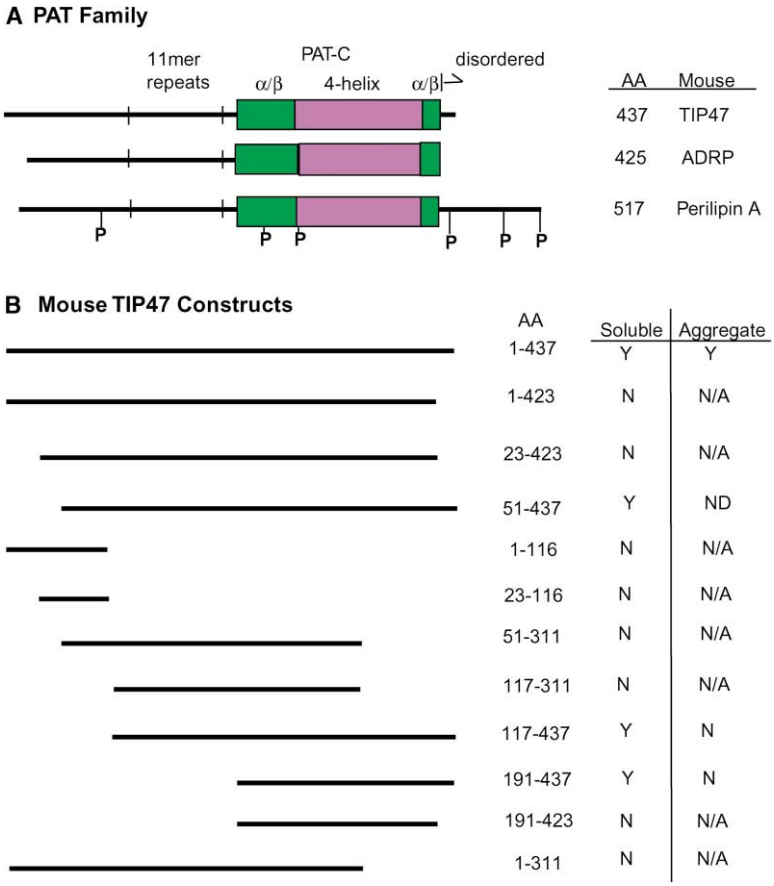

Figure 1. Domain Structure of PAT Proteins

(A) Domain structure. The PAT-C region is shown in filled rectangles, green for the α/β domain, magenta for the four-helix bundle domain. The 11-mer repeat regions are delineated by vertical bars at the N- and C terminus of the repeat region. PKA phosphorylation sites are denoted by the letter "P."

(B) Constructs used in this study. N/A, not applicable, ND, not determined.

Table 1. Crystallographic Data, Phasing, and Refinement Statistics

	Native	KI	$HgCl_2$	K_2PtCl_4
Data Collection and Phasing				
Space group	$P6_322$	$P6_322$	$P6_322$	$P6_322$
Unit cell	a =b = 118.7 Å, c = 97.3 Å	a =b = 118.6 Å, c = 97.6 Å	a =b = 118.5 Å, c = 96.9 Å	a =b = 118.1 Å, c = 97.5 Å
Resolution	2.8 Å	3.0 Å	3.0 Å	3.2 Å
R_{merge}[a]	0.069	0.121	0.077	0.068
Completeness	99.9	99.9	95.2	98.5
Unique reflections	10,450	8564	8108	6942
Phasing power[b]		0.48	0.58	0.60
No. sites		5	2	3
Figure of merit[c]	0.40			
Refinement				
R_{work}[d]	0.236			
R_{free}[e]	0.272			
Cross-validated Luzzati error	0.49 Å			
Rmsd, bonds	0.008 Å			
Rmsd, angles	1.1°			
Mean B	55.4 $Å^2$			
Wilson B	54.9 $Å^2$			
Protein atoms	1505			
Solvent atoms	0			
βME atoms	4			

[a] $R_{merge} = \Sigma|I(k) - <I(k)>|/\Sigma I(k)$.

[b] Phasing power is $\Sigma|F_H|/\Sigma|E_{rms}|$ for acentric reflections, where E is the lack of closure.

[c] MIRAS figure of merit prior to density modification.

[d] $R_{work} = \Sigma|F_{obs} - kF_{calc}|/\Sigma|F_{obs}|$ summed over all reflections used in refinement.

[e] R_{free} is the R value calculated for a test set of reflections, comprising a randomly selected 5% of the data, not used during refinement.

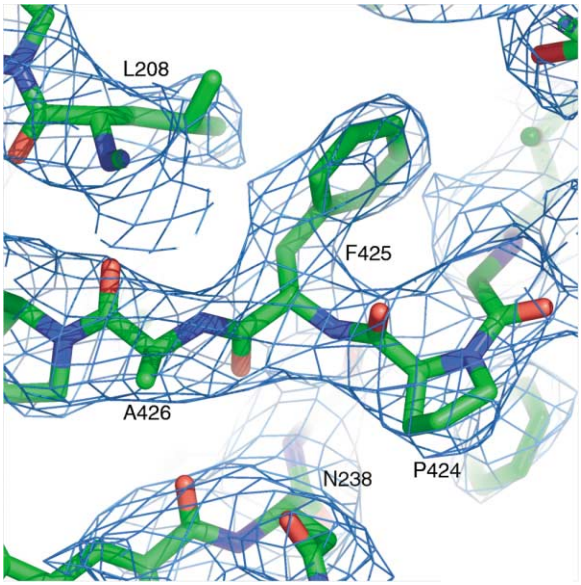

Figure 2. MIRAS Electron Density

Electron density calculated by density modification of MIRAS synthesis, contoured at 1.0 σ, and displayed in PYMOL. The refined model is juxtaposed with the density in the region of Phe-425.

the widest gap between the domains, 18 Å long, and 10 Å deep. On the four-helix bundle side of the cleft, the wall is formed by hydrophobic residues from the first two helices in the bundle: Ser-258, Leu-262, Ala-265, Ala-347, Leu-348, Ser-351, and the aliphatic portions of the side-chains of Lys-261 and Gln-353 (Figures 5 and 6). On the α/β domain side, the corresponding wall of the cleft is formed by Pro-222, Phe-240, Pro-424, and Phe-425. The floor of the cleft is formed by Trp-420, Leu-421, and Val-422, which are at the junction between the two domains. Aside from this cleft, there is little to distinguish the surface of the four-helix bundle domain. The α/β domain has three prominently exposed hydrophobic side chains: Leu-217, Met-227, and Met-419. All three are located on the same face of the domain, which is distal to the four-helix bundle domain.

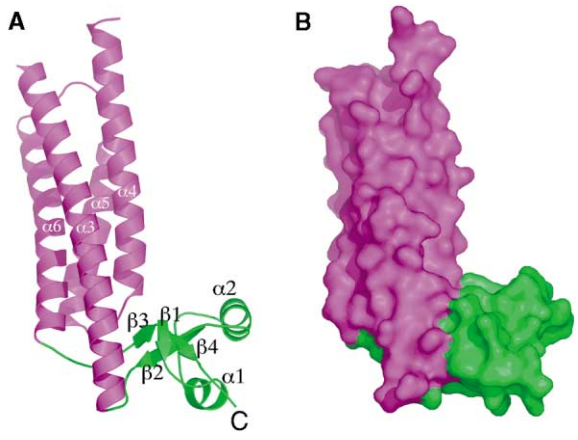

Figure 3. Overall Structure of TIP47 PAT-C

The domains are colored as in Figure 1.

Structural Homologies

We searched the Protein Data Bank for structural similarity to PAT-C using the VAST and Dali search tools (Gibrat et al., 1996; Holm and Sander, 1995). Many four-helix bundle proteins were identified as high-scoring matches in both searches, while no α/β proteins were identified. Subsequent searches using only the isolated α/β domain yielded no matches. This suggests that the PAT-C α/β domain is structurally unique, albeit with the caveat that scoring schemes for matches can be less reliable for small substructures. The high-scoring matches to the four-helix bundle domain include α-catenin, the oxygen evolving protein oee3, cytochrome c, CheA, myohemerythrin, the aspartate receptor tar, the vinculin tail domain, and the LDL-receptor binding domain of apolipoprotein E (Figure 7).

Discussion

Function of the PAT-C Domains

The PAT-C structure contains only one striking surface feature, a deep hydrophobic cleft between the α/β and four-helix bundle domains. The hydrophobic character of the residues that map to the cleft floor and walls is highly conserved between the TIP47 and ADRP sequences, and partly conserved between the TIP47 and perilipin sequences (Figure 6). The deep cleft is not suggestive of an extended phospholipid membrane or hydrocarbon droplet binding site. The shape, size, and hydrophobicity of the cleft are, however, consistent with binding to a hydrophobic peptide, protein, or a small molecule such as a monomeric lipid. The hydrophobic cleft is rimmed by basic residues, which contribute to a strong electropositive potential in the vicinity. The presence of this cleft as a central, conserved structural feature suggests that it is functionally important.

The CD-MPR and HIV gp41 interact with TIP47 through a diaromatic motif (Blot et al., 2003; Krise et al., 2000; Orsel et al., 2000) and the cleft is a likely site for this interaction. In an attempt to identify the interacting site, we synthesized diaromatic motif-containing peptides corresponding to the TIP47 binding sequences of the CD-MPR and of HIV gp41. Attempts to obtain the structure of a diaromatic peptide/TIP47 complex were hindered by the insolubility of the peptides in water. We dissolved the gp41 peptide in DMSO and determined the structure of TIP47 soaked in a peptide/DMSO/water mixture, but detected no significant structure factor differences nor any new electron density features (data not shown). These results could be due either to a lack of interaction with the domain or to precipitation upon dilution of the peptide/DMSO solution into the crystallization solution. ADRP does not interact with the CD-MPR. Despite the high conservation of the protein overall and in the cleft region, there are a few sequence differences in this area between ADRP and TIP47 that might be consistent with a difference in ligand specificity. Because the pocket is so well conserved between ADRP and TIP47, we postulate that there is a common function for this pocket in all PAT proteins, in addition to the probable MPR binding function in TIP47. It will be important to determine whether this pocket is the locus for fatty acid and sterol binding to ADRP. Based

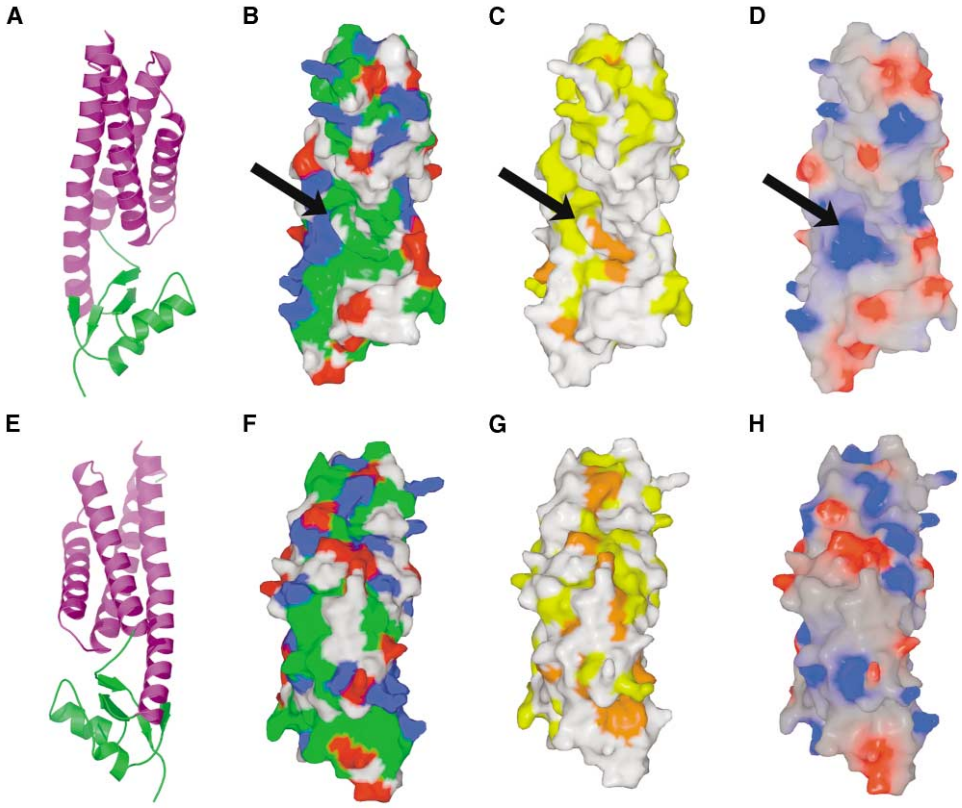

Figure 4. Molecular Surface of PAT-C

(A and E) Secondary structures shown as a guide to the orientation of the surfaces.

(B and F) The surface is colored blue for basic residues (Lys, Arg, His), red for acidic residues (Asp, Glu), green for hydrophobic residues (Ala, Gly, Pro, Val, Ile, Leu, Phe, Tyr, Trp, Cys, Met), and white for uncharged polar residues (Thr, Ser, Gln, Asn).

(C and G) The surface is colored orange where the residues property (basic, acidic, or hydrophobic) is conserved in at least five out of the six PAT proteins shown in Figure 6; yellow if the property is conserved in three PAT proteins out of the six shown.

(D and H) Surface is colored by electrostatic potential, with saturating blue and red at a potential of +10 kT/e and −10 kT/e, respectively. The hydrophobic cleft is marked by an arrow in (B)–(D).

on the similarity of many of the aligned residues in TIP47 and perilipin, we propose that the cleft is also present in all PAT proteins, regardless of species. If the site were as functionally important as we propose, it raises the exciting possibility that small molecule drugs could be developed that would functionally inactivate perilipin and, thus, phenocopy the leanness of the *peri*$^{-/-}$ mice.

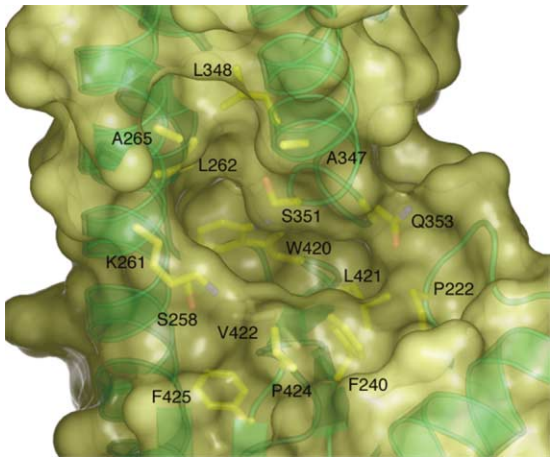

Figure 5. The Hydrophobic Cleft

Side chains of residues forming the floor and walls of the cleft are shown under a transparent molecular surface.

Recruitment, Regulation, and Targeting Mechanisms

Perilipin plays a critical role in regulating hormone-sensitive lipolysis by recruiting HSL to lipid droplets. PKA phosphorylation of both HSL and perilipin are required for HSL recruitment to droplets (Su et al., 2003; Sztalryd et al., 2003). ADRP will not replace this function of perilipin (Sztalryd et al., 2003). There are six phosphorylated Ser residues in mouse perlipin A: 81, 222, 276, 433, 492, and 517. On a group-wise basis, the first three have a demonstrated role in both lipolysis mediated by HSL (Souza et al., 2002; Sztalryd et al., 2003) and by other lipases (Tansey et al., 2003). The individual roles of the sites have yet to be determined (Zhang et al., 2003). The second and third sites are within the ordered PAT-C region. Murine peri-A Ser-222 corresponds to TIP47 Ser-245. This Ser is solvent exposed and located just before the first junction between the α/β domain and the four-helix bundle, in the linker preceding the first helix in

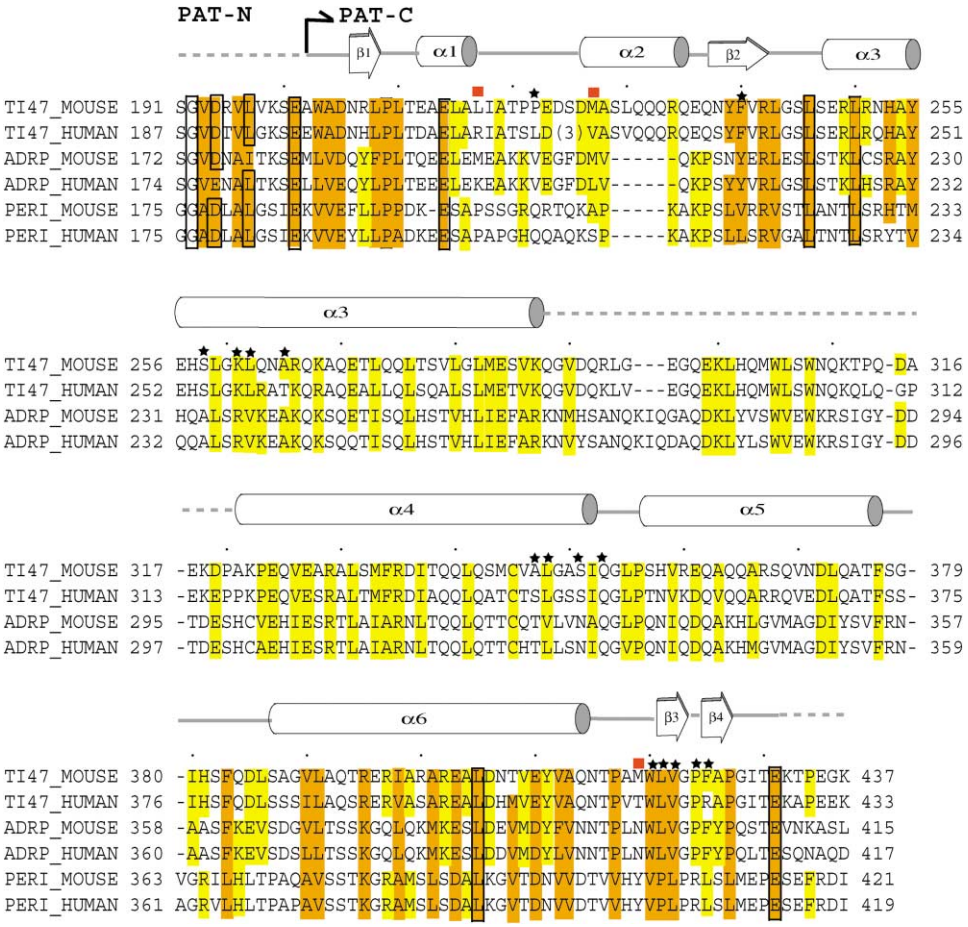

Figure 6. Structure and Sequence Alignment of PAT-C Regions

The sequence is marked at 10 residue intervals according to mouse TIP47 numbering. Red boxes above the alignment mark exposed hydrophobic residues on the surface of the α/β domain distal to the helical bundle, and stars mark hydrophobic cleft residues. Outlined boxes surround residues that are identical in at least five out of the six PAT proteins shown. Shaded boxes are colored as in Figure 4C. The alignment is taken from the Pfam database (Bateman et al., 2002) and modified to eliminate gaps within secondary structural elements. When it became apparent from the structure that the entire α/β domain was a single conserved unit, 21 residues were manually appended to the Pfam alignment corresponding to the C-terminal portion of this domain. The sequence similarity between perilipin and the other PAT proteins is low from residues 234 to 362 (mouse numbering), and the alignment in this region has been omitted.

the bundle, α3. This places the Ser on the same face of the α/β domain as the exposed hydrophobic side chains mentioned above. Murine perilipin-A Ser-276 corresponds roughly to the disordered region between α3 and α4, at the tip of the four-helix bundle most distal to the α/β domain. Either one of these exposed sites could regulate HSL translocation, either directly or indirectly, by altering interdomain interactions between the PAT-N and PAT-C regions.

The mechanism of targeting to lipid droplets is one of the most pressing questions in the PAT protein field. The intact PAT-C region of ADRP is cytosolic (Nakamura and Fujimoto, 2003), suggesting that the folded PAT-C structure is not by itself a targeting determinant. Constructs corresponding to fragments of the PAT-C structure can target perilipin (Garcia et al., 2003; Zhang et al., 2003) and ADRP (McManaman et al., 2003; Nakamura and Fujimoto, 2003; Targett-Adams et al., 2003) to lipid droplets. PAT-C fragments have also been shown to mistarget to the mitochondrion (Nakamura and Fujimoto, 2003). Given our new understanding that the PAT-C region folds into a single structural unit, caution is needed in interpreting these fragment-based targeting studies. The PAT-C domain contains a series of amphipathic helices that would normally be folded into the structure and unavailable for membrane association. However, these helices may become surface exposed in subfragments of PAT-C and capable of targeting to any available membrane, including lipid droplets, the mitochondrial membrane, or elsewhere. Conversely, the presence of a partial PAT-C structure could lead to misfolding of the remainder of the protein, and thereby abrogate targeting.

Constructs containing the PAT-N regions associate strongly with intracellular lipid doplets. The PAT-N regions contain repeats that were first identified as 33-mers in the plasma membrane-associated protein S3-12 (Scherer et al., 1998), which is homologous to the PAT-N region of the PAT proteins (Londos et al., 1999). These repeats were subsequently found to have an 11-

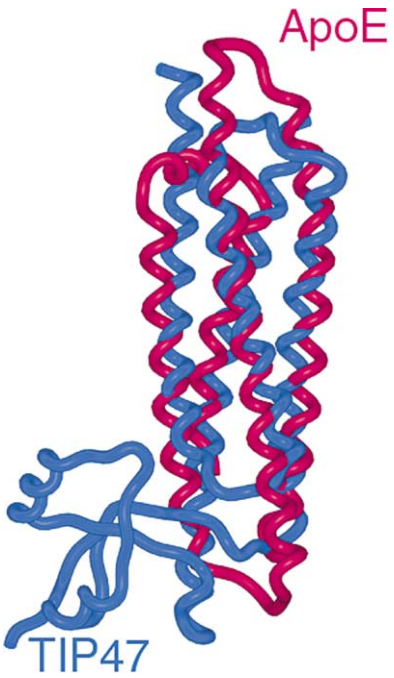

Figure 7. Structural Similarity of TIP47, Residues 206–431, and Apolipoprotein E, Residues 23–166

mer repeat substructure (Bussell and Eliezer, 2003). Such 11-mer are present in many other lipid-associated or membrane-associated proteins, including synucleins, apolipoproteins, phosphate cytidyltransferases, dehydrins, and S3-12 (Bussell and Eliezer, 2003). The repeats regions of many of these proteins, including α-synuclein (Davidson et al., 1998), apolipoprotein A-I (Segrest et al., 1999, 2000), late embryogenesis abundant protein D-11 (Koag et al., 2003), and cytidyltransferase (Dunne et al., 1996), have been found to directly bind lipids. The similarity of the 11-mer repeats in PAT proteins to the repeats in other lipid binding proteins suggests that the PAT 11-mers are likely to be an important locus for lipid binding, although this has yet to be tested directly.

Parallels between Lipid Droplet Proteins and Apolipoproteins

The structural and deletion analysis of TIP47 provides, for the first time, a three-dimensional template for understanding PAT proteins. The PAT-C region consists of two domains, one novel, and one similar to many other four-helix bundle proteins. There is little to differentiate the quality of the fit to various known four-helix bundle structures. Of the top ten matches as scored by Dali, the apolipoprotein E N-terminal domain (Wilson et al., 1991) has the clearest functional relationship with the PAT proteins. The structures can be superimposed upon each other with a rmsd of 2.5 Å over 89 Cα positions out of a total of 144 residues in the apoE fragment. The N-terminal domain of apoE interacts with the LDL receptor in the presence of phospholipids, but has a low affinity for lipids on its own (Saito et al., 2001). The primary function of the apoE N-terminal (four-helical bundle) domain seems to be protein:protein interaction. In contrast, the C-terminal domain of apoE, which is predicted to be an amphipathic helix and to lack a defined tertiary fold, has a high affinity for phospholipids and is thought to provide the primary driving force for protein:lipid interaction (Saito et al., 2001).

The similarity between the PAT-N 11-mer repeats and Apo A, and the PAT-C structure and the N-terminal domain of Apo E draws inescapable parallels between PAT family lipid droplet proteins and apolipoproteins. The sequence similarities are distant enough to leave uncertain whether they arose by convergent or divergent evolution; but the functional analogy is clear. It is scarcely surprising to discover a close structural relationship between lipid droplet coating proteins and apolipoproteins. The lipidic component of both droplets and lipoprotein particles consists of a triglyceride and cholesterol core surrounded by a phospholipid monolayer. The functions of the associated proteins are analogous: to stabilize assembly, to provide docking sites for the appropriate receptors and regulatory proteins, and to regulate access to the underlying lipids. Apolipoproteins have been studied intensively for decades, while the field of lipid droplet associated proteins has emerged over only the past decade or so. The link having been established, the extant biochemistry and biophysics of apolipoproteins provides a rich conceptual foundation for further experimentation in the lipid droplet protein field.

Experimental Procedures

Protein Expression and Purification

Twelve different truncations of TIP47 were screened for soluble protein expression. The four constructs that contained the full C terminus were all found to be soluble. The TIP47 PAT-C domain (Δ1-190) was selected for crystal screening because it was stable throughout the purification process. The TIP47 PAT-C domain was subcloned into the pHIS-parallel2 vector (Sheffield et al., 1999). Overexpression of the His_6-tagged protein in *Escherichia coli* BL21-CodonPlus (DE3)-RIL cells (Stratagene, La Jolla, CA) was induced with isopropyl-β-D-thiogalactoside at 20°C. The protein was purified by using a Ni^{2+}-nitrilotriacetate (NTA) column equilibrated with 50 mM Tris•HCl, (pH 8), 300 mM NaCl, 10 mM imidazole, 1 mM β-mercaptoethanol (βME) and eluted using an imidazole gradient and a FPLC system (Amersham Pharmacia). The His_6 tag was removed with TEV protease and the protein was subjected to a second purification with the Ni^{2+}-NTA resin (Qiagen, Valencia, CA). The protein was further purified on a Superdex 200 prep grade gel filtration column (Amersham Biosciences, Piscataway, NJ) equilibrated with 50 mM Tris•HCl, (pH 8), 300 mM NaCl, 10 mM DTT, 0.5 mM EDTA and attached to a FPLC system. The cleaved protein contains the vector-derived sequence GAMGS followed by the TIP47 PAT-C residues 191–437. The protein was stored at −80°C in elution buffer and 10% glycerol.

Crystallization, X-Ray Diffraction Data Collection, and Structure Determination

The protein was dialyzed into 50 mM Tris•HCl (pH 8), 300 mM NaCl, 10 mM DTT, 0.5 mM EDTA for crystallization. Initial crystallization conditions were found by using the Emerald Biostructures (Bainbridge Island, WA) Wizard I & II screens, and then optimized. A hanging droplet consisting of 10 μl of the protein solution (18 mg/ml) mixed with 7 μl of the reservoir solution containing 0.8 M Na citrate, 0.1 M Tris•HCl (pH 8.5), 0.2 M NaCl was equilibrated against 0.5 ml of the reservoir solution. Crystals suitable for data collection (see Table 1) grew within a month at 20°C to ≈200 μm maximum dimension. Native crystals were cryoprotected by soaking for 10 s in 1M Na citrate, 0.1 M Tris•HCl (pH 8.5), 0.2 M NaCl, 25% glycerol.

They were then immediately frozen under N_2 vapor at 95 K. Heavy atom derivatives were prepared as follows. An iodide derivative (Dauter and Dauter, 2001) was prepared by a 2 min soak in 1 M KI, 1 M Na-citrate, 0.1 M Tris (pH 8.5), 0.2 M NaCl, 25% glycerol. A $HgCl_2$ derivative was prepared by a quick soak (Sun et al., 2002) for 10 min in 1 mM $HgCl_2$, 1 M Na citrate, 0.1 M Tris•HCl (pH 8.5), 0.2 M NaCl, followed by 10 s soak in the glycerol cryoprotectant, and frozen. A chloroplatinate derivative was prepared by a 10 min soak in 10 mM K_2PtCl_4, 1 M sodium citrate, 0.1 M Tris•HCl (pH 8.5), 0.2 M sodium chloride, followed by 10 s soak in the glycerol cryoprotectant. Data collection was performed using an Raxis-IV detector and a Rigaku rotating anode X-ray generator, and data were processed with HKL2000 (HKL Research, Charlottesville, VA). Heavy atom binding sites were located in a simultaneous search of all three derivatives using SOLVE (Terwilliger and Berendzen, 1999). An electron density map was calculated at 3.0 Å using isomorphous and anomalous differences for phasing, and modified using RESOLVE (Terwilliger, 2000). The structure was modeled using O (Jones et al., 1991) and refined using torsional dynamics and the maximum likelihood target function in CNS (Brunger et al., 1998) and subsequently in Refmac5 (Murshudov et al., 1997).

Acknowledgments

We thank A. Hickman, R. Akhavan, R. Trievel, B. Beach, S. Misra, G. Miller, and D. Clark for helpful advice; S. Sechi for assistance with mass spectrometry; B. Canagarajah for computational support; D. Agard, D. Eliezer, and D. Small for discussions; and J. Bonifacino and C. Arighi for comments on the manuscript.

Received: March 8, 2004
Revised: April 5, 2004
Accepted: April 6, 2004
Published: July 13, 2004

References

Atshaves, B.P., Storey, S.M., McIntosh, A.L., Petrescu, A.D., Lyuksyutova, O.I., Greenberg, A.S., and Schoroeder, F. (2001). Sterol carrier protein-2 expression modulates protein and lipid composition of lipid droplets. J. Biol. Chem. *276*, 25324–25335.

Barbero, P., Buell, E., Zulley, S., and Pfeffer, S.R. (2001). TIP47 is not a component of lipid droplets. J. Biol. Chem. *276*, 24348–24351.

Bateman, A., Birney, E., Cerruti, L., Durbin, R., Etwiller, L., Eddy, S.R., Griffiths-Jones, S., Howe, K.L., Marshall, M., and Sonnhammer, E.L.L. (2002). The Pfam protein families database. Nucleic Acids Res. *30*, 276–280.

Blot, G., Janvier, K., Le Panse, S., Benarous, R., and Berlioz-Torrent, C. (2003). Targeting of the human immunodeficiency virus type 1 envelope to the trans-Golgi network through binding to TIP47 is required for Env incorporation into virions and infectivity. J. Virol. *77*, 6931–6945.

Brasaemle, D.L., Barber, T., Wolins, N.E., Serrero, G., Blanchette-Mackie, E.J., and Londos, C. (1997). Adipose differentiation-related protein is an ubiquitously expressed lipid storage droplet-associated protein. J. Lipid Res. *38*, 2249–2263.

Brasaemle, D.L., Rubin, B., Harten, I.A., Gruia-Gray, J., Kimmel, A.R., and Londos, C. (2000). Perilipin A increases triacylglycerol storage by decreasing the rate of triacylglycerol hydrolysis. J. Biol. Chem. *275*, 38486–38493.

Brown, D.A. (2001). Lipid droplets: proteins floating on a pool of fat. Curr. Biol. *11*, R446–R449.

Brunger, A.T., Adams, P.D., Clore, G.M., DeLano, W.L., Gros, P., Grosse-Kunstleve, R.W., Jiang, J.S., Kuszewski, J., Nilges, M., Pannu, N.S., et al. (1998). Crystallography & NMR system: a new software suite for macromolecular structure determination. Acta Crystallogr. D Biol. Crystallogr. *54*, 905–921.

Bussell, R., and Eliezer, D. (2003). A structural and functional role for 11-mer repeats in alpha-synuclein and other exchangeable lipid binding proteins. J. Mol. Biol. *329*, 763–778.

Dauter, Z., and Dauter, M. (2001). Entering a new phase: using solvent halide ions in protein structure determination. Structure *9*, R21–R26.

Davidson, W.S., Jonas, A., Clayton, D.F., and George, J.M. (1998). Stabilization of alpha-synuclein secondary structure upon binding to synthetic membranes. J. Biol. Chem. *273*, 9443–9449.

Diaz, E., and Pfeffer, S.R. (1998). TIP47: a cargo selection device for mannose 6-phosphate receptor trafficking. Cell *93*, 433–443.

Dunne, S.J., Cornell, R.B., Johnson, J.E., Glover, N.R., and Tracey, A.S. (1996). Structure of the membrane binding domain of CTP:phosphocholine cytidylyltransferase. Biochemistry. *35*, 11975–11984.

Garcia, A., Sekowski, A., Subramanian, V., and Brasaemle, D.L. (2003). The central domain is required to target and anchor perilipin A to lipid droplets. J. Biol. Chem. *278*, 625–635.

Gibrat, J.F., Madej, T., and Bryant, S.H. (1996). Surprising similarities in structure comparison. Curr. Opin. Struct. Biol. *6*, 377–385.

Gronke, S., Beller, M., Fellert, S., Ramakrishnan, H., Jackle, H., and Kuhnlein, R.P. (2003). Control of fat storage by a Drosophila PAT domain protein. Curr. Biol. *13*, 603–606.

Holm, L., and Sander, C. (1995). Dali—a network tool for protein-structure comparison. Trends Biochem. Sci. *20*, 478–480.

Jones, T.A., Zou, J.Y., Cowan, S.W., and Kjeldgaard, M. (1991). Improved methods for building protein models in electron-density maps and the location of errors in these models. Acta Crystallogr. A *47*, 110–119.

Koag, M.C., Fenton, R.D., Wilkens, S., and Close, T.J. (2003). The binding of maize DHN1 to lipid vesicles. Gain of structure and lipid specificity. Plant Physiol. *131*, 309–316.

Krise, J.P., Sincock, P.M., Orsel, J.G., and Pfeffer, S.R. (2000). Quantitative analysis of TIP47-receptor cytoplasmic domain interactions: implications for endosome-to-trans Golgi network trafficking. J. Biol. Chem. *275*, 25188–25193.

Londos, C., Brasaemle, D.L., Schultz, C.J., Segrest, J.P., and Kimmel, A.R. (1999). Perilipins, ADRP, and other proteins that associate with intracellular neutral lipid droplets in animal cells. Semin. Cell Dev. Biol. *10*, 51–58.

Lu, X.Y., Gruia-Gray, J., Copeland, N.G., Gilbert, D.J., Jenkins, N.A., Londos, C., and Kimmel, A.R. (2001). The murine perilipin gene: the lipid droplet-associated perilipins derive from tissue-specific, mRNA splice variants and define a gene family of ancient origin. Mamm. Genome *12*, 741–749.

Martinez-Botas, J., Anderson, J.B., Tessier, D., Lapillonne, A., Chang, B.H.J., Quast, M.J., Gorenstein, D., Chen, K.H., and Chan, L. (2000). Absence of perilipin results in leanness and reverses obesity in Lepr db db mice. Nat. Genet. *26*, 474–479.

McManaman, J.L., Zabaronick, W., Schaack, J., and Orlicky, D.J. (2003). Lipid droplet targeting domains of adipophilin. J. Lipid Res. *44*, 668–673.

Medigeshi, G.R., and Schu, P. (2003). Characterization of the in vitro retrograde transport of MPR46. Traffic *4*, 802–811.

Miura, S., Gan, J.W., Brzostowski, J., Parisi, M.J., Schultz, C.J., Londos, C., Oliver, B., and Kimmel, A.R. (2002). Functional conservation for lipid storage droplet association among perilipin, ADRP, and TIP47 (PAT)-related proteins in mammals, Drosophila, and Dictyostelium. J. Biol. Chem. *277*, 32253–32257.

Murshudov, G.N., Vagin, A.A., and Dodson, E.J. (1997). Refinement of macromolecular structures by the maximum-likelihood method. Acta Crystallogr. D Biol. Crystallogr. *53*, 240–255.

Nakamura, N., and Fujimoto, T. (2003). Adipose differentiation-related protein has two independent domains for targeting to lipid droplets. Biochem. Biophys. Res. Commun. *306*, 333–338.

Ohashi, M., Mizushima, N., Kabeya, Y., and Yoshimori, T. (2003). Localization of mammalian NAD(P)H steroid dehydrogenase-like protein on lipid droplets. J. Biol. Chem. *278*, 36819–36829.

Orsel, J.G., Sincock, P.M., Krise, J.P., and Pfeffer, S.R. (2000). Recognition of the 300-kDa mannose 6-phosphate receptor cytoplasmic domain by 47-kDa tail-interacting protein. Proc. Natl. Acad. Sci. USA *97*, 9047–9051.

Rost, B., and Liu, J.F. (2003). The PredictProtein server. Nucleic Acids Res. *31*, 3300–3304.

Saito, H., Dhanasekaran, P., Baldwin, F., Weisgraber, K.H., Lund-Katz, S., and Phillips, M.C. (2001). Lipid binding-induced conformational change in human apolipoprotein E: evidence for two lipid-bound states on spherical particles. J. Biol. Chem. *276*, 40949–40954.

Scherer, P.E., Bickel, P.E., Kotler, M., and Lodish, H.F. (1998). Cloning of cell-specific secreted and surface proteins by subtractive antibody screening. Nat. Biotechnol. *16*, 581–586.

Schultz, C.J., Torres, E., Londos, C., and Torday, J.S. (2002). Role of adipocyte differentiation-related protein in surfactant phospholipid synthesis by type II cells. Am. J. Physiol. Lung Cell Mol. Physiol. *283*, L288–L296.

Segrest, J.P., Jones, M.K., Klon, A.E., Sheldahl, C.J., Hellinger, M., De Loof, H., and Harvey, S.C. (1999). A detailed molecular belt model for apolipoprotein A-I in discoidal high density lipoprotein. J. Biol. Chem. *274*, 31755–31758.

Segrest, J.P., Li, L., Anantharamaiah, G.M., Harvey, S.C., Liadaki, K.N., and Zannis, V. (2000). Structure and function of apolipoprotein A-I and high-density lipoprotein. Curr. Opin. Lipidol. *11*, 105–115.

Serrero, G., Frolov, A., Schroeder, F., Tanaka, K., and Gelhaar, L. (2000). Adipose differentiation related protein: expression, purification of recombinant protein in Escherichia coli and characterization of its fatty acid binding properties. Biochim. Biophys. Acta *1488*, 245–254.

Sheffield, P., Garrard, S., and Derewenda, Z. (1999). Overcoming expression and purification problems of RhoGDI using a family of "parallel" expression vectors. Protein Expr. Purif. *15*, 34–39.

Sincock, P.M., Ganley, I.G., Krise, J.P., Diederichs, S., Sivars, U., O'Connor, B., Ding, L., and Pfeffer, S.R. (2003). Self-assembly is important for TIP47 function in mannose 6- phosphate receptor transport. Traffic *4*, 18–25.

Souza, S.C., de Vargas, L.M., Yamamoto, M.T., Lien, P., Franciosa, M.D., Moss, L.G., and Greenberg, A.S. (1998). Overexpression of perilipin A and B blocks the ability of tumor necrosis factor alpha to increase lipolysis in 3T3–L1 adipocytes. J. Biol. Chem. *273*, 24665–24669.

Souza, S.C., Muliro, K.V., Liscum, L., Lien, P., Yamamoto, M.T., Schaffer, J.E., Dallal, G.E., Wang, X.Z., Kraemer, F.B., Obin, M., et al. (2002). Modulation of hormone-sensitive lipase and protein kinase A-mediated lipolysis by perilipin A in an adenoviral reconstituted system. J. Biol. Chem. *277*, 8267–8272.

Su, C.L., Sztalryd, C., Contreras, J.A., Holm, C., Kimmel, A.R., and Londos, C. (2003). Mutational analysis of the hormone-sensitive lipase translocation reaction in adipocytes. J. Biol. Chem. *278*, 43615–43619.

Sun, P.D., Radaev, S., and Kattah, M. (2002). Generating isomorphous heavy-atom derivatives by a quick-soak method. Part I: test cases. Acta Crystallogr. D Biol. Crystallogr. *58*, 1092–1098.

Sztalryd, C., Xu, G.H., Dorward, H., Tansey, J.T., Contreras, J.A., Kimmel, A.R., and Londos, C. (2003). Perilipin A is essential for the translocation of hormone-sensitive lipase during lipolytic activation. J. Cell Biol. *161*, 1093–1103.

Tansey, J.T., Huml, A.M., Vogt, R., Davis, K.E., Jones, J.M., Fraser, K.A., Brasaemle, D.L., Kimmel, A.R., and Londos, C. (2003). Functional studies on native and mutated forms of perilipins: a role in protein kinase A-mediated lipolysis of triacylglycerols in Chinese hamster ovary cells. J. Biol. Chem. *278*, 8401–8406.

Tansey, J.T., Sztalryd, C., Gruia-Gray, J., Roush, D.L., Zee, J.V., Gavrilova, O., Reitman, M.L., Deng, C.X., Li, C., Kimmel, A.R., et al. (2001). Perilipin ablation results in a lean mouse with aberrant adipocyte lipolysis, enhanced leptin production, and resistance to diet-induced obesity. Proc. Natl. Acad. Sci. USA *98*, 6494–6499.

Targett-Adams, P., Chambers, D., Gledhill, S., Hope, R.G., Coy, J.F., Girod, A., and McLauchlan, J. (2003). Live cell analysis and targeting of the lipid droplet-binding adipocyte differentiation-related protein. J. Biol. Chem. *278*, 15998–16007.

Terwilliger, T.C. (2000). Maximum-likelihood density modification. Acta Crystallogr. D Biol. Crystallogr. *56*, 965–972.

Terwilliger, T.C., and Berendzen, J. (1999). Automated MAD and MIR structure solution. Acta Crystallogr. D Biol. Crystallogr. *55*, 849–861.

Wilson, C., Wardell, M.R., Weisgraber, K.H., Mahley, R.W., and Agard, D.A. (1991). Three-dimensional structure of the LDL receptor-binding domain of human apolipoprotein-E. Science *252*, 1817–1822.

Wolins, N.E., Rubin, D., and Brasaemle, D.L. (2001). TIP47 associates with lipid droplets. J. Biol. Chem. *276*, 5101–5108.

Zhang, H.H., Souza, S.C., Muliro, K.V., Kraemer, F.B., Obin, M.S., and Greenberg, A.S. (2003). Lipase-selective functional domains of perilipin A differentially regulate constitutive and protein kinase A-stimulated lipolysis. J. Biol. Chem. *278*, 51535–51542.

Accession Numbers

The coordinates have been deposited with the Protein Data Bank at the RCSB with accession 1SZI.